Journal Pre-proof

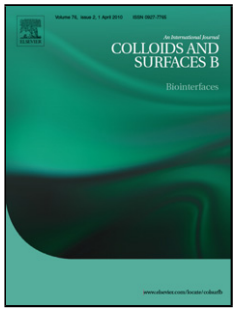

Assessing 3D printing of Poly(ether-ether-ketone) and cellular cHAp to increase biointerfaces as a biomedical material

Bankole I. Oladapo, S. Abolfazl Zahedi, Sikiru O. Ismail

PII: S0927-7765(21)00170-3

DOI: https://doi.org/10.1016/j.colsurfb.2021.111726

Reference: COLSUB 111726

To appear in: *Colloids and Surfaces B: Biointerfaces*

Received Date: 20 January 2021

Revised Date: 11 March 2021

Accepted Date: 24 March 2021

Please cite this article as: Oladapo BI, Zahedi SA, Ismail SO, Assessing 3D printing of Poly(ether-ether-ketone) and cellular cHAp to increase biointerfaces as a biomedical material, *Colloids and Surfaces B: Biointerfaces* (2021), doi: https://doi.org/10.1016/j.colsurfb.2021.111726

Assessing 3D printing of Poly(ether-ether-ketone) and cellular cHAp to increase biointerfaces as a biomedical material

Bankole I. Oladapo[a*], S. Abolfazl Zahedi[a], Sikiru O.Ismail[b]

[a]*School of Engineering and Sustainable Development, De Montfort University, UK*
[b]*Engineering and Computer Science, University of Hertfordshire, UK*

**Corresponding author: E-mail: bankolyable01@gmail.com*

Graphical Abstract

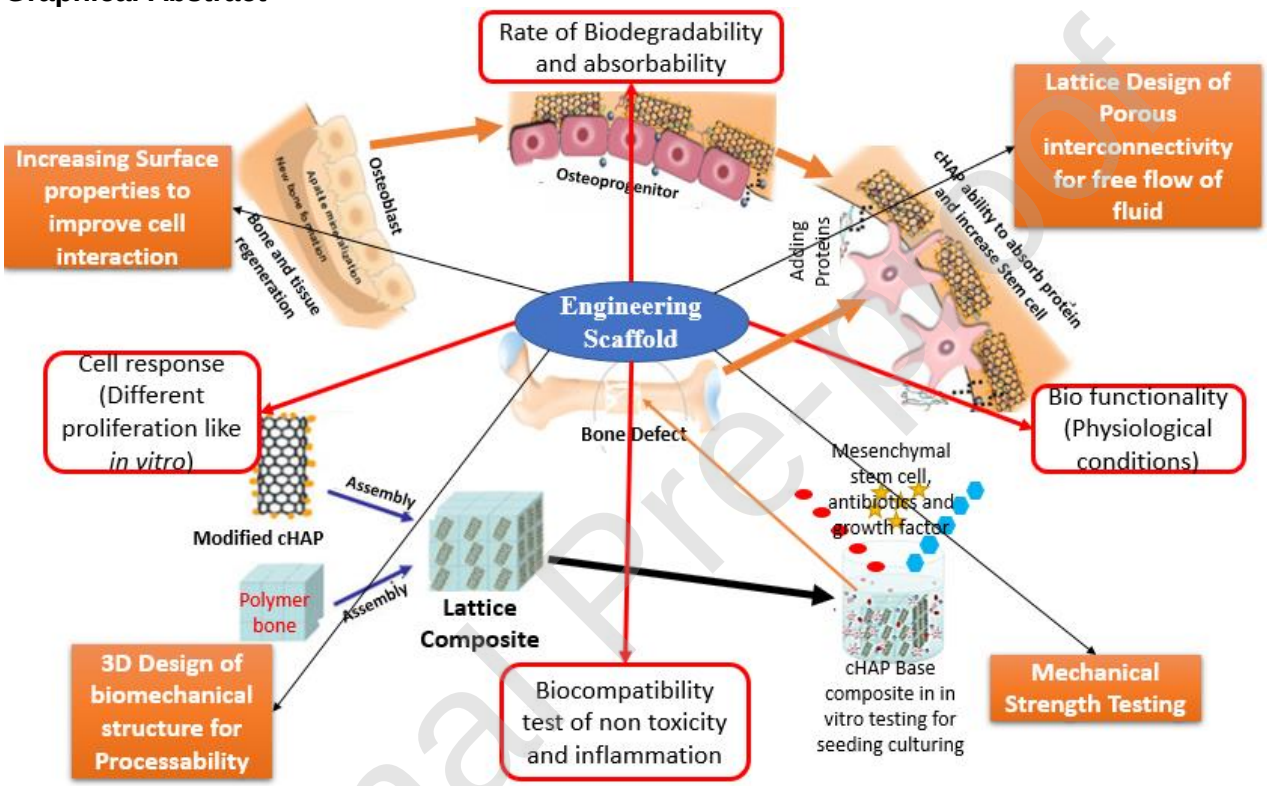

Highlight

- Evaluations of structural 3D printability of PEEK for a range of biomedical applications.
- Highlights the best optimum 3D printer for processing PEEK/cHAp composite in different forms
- Current printing problems, and potential applications of 3D printing of PEEK-cHAP in the medical implants.
- Study proposes an analytical review on the 3D printing of PEEK/cHAP and its composite,
- Ideas, feasible solutions, and enabling scientific mechanisms to improve the 3D printability of PEEK/HAp.

Abstract

Polyetheretherketone (PEEK) is a polymer with better lignin biocompatibility than other polymers and useful biomedical engineering applications. This research summarises the outcomes of an evaluation conducted on PEEK material composites such as cellular calcium hydroxyapatite (CHAp) for medical applications. PEEK's prospects for the medical implant are highlighted, and critical analysis and review is presented of 3D printing of PEEK and CHAp and their biological macromolecular behaviours. An electronic search is carried out of Scupos database, Google search and peer-reviewed papers published in the last ten years. Because of the extraordinary strength and biological behaviour of PEEK and its composite CHAp, 3D printed PEEK has several biomedical applications, and it is biological macromolecular behaviour leads to health sustainability. This work highlights its biological macromolecular behaviour as a bone implant material and the optimum 3D printing process for PEEK and CHAp for medical applications. The current problems with printing PEEK and CHAp are investigated along with their possible uses. Possible solutions to improve the 3D printability of PEEK and CHAp are explained based on scientific mechanisms. This detailed report benefits both the scientific community and the medical industry to enhance 3D printing concepts for PEEK and CHAp.

Keyword: PEEK; 3D printing; Cellular CHAp; Biomaterial; Bone implant

Abbreviations

HAp	Hydroxyapatite	PEEK	Polyetheretherketone
ISO	International Organization for Standardisation	PLIF	Posterior lumbar interbody fusion
OH	Hydroxyl	Tg	Glass transition temperature
OHA	Partially dehydroxylated	Tm	Melting temperature
β-TCP	Beta-tricalcium phosphate	TTCP	Tetracalcium phosphate
3D	Three-dimensional	α-TCP	Alpha-tricalcium phosphate

1. Introduction

An implant is any medical device developed by humans to replace or assist the regeneration of the human body's biological macromolecular structure. The use of implants began with autologous implants, made of natural materials taken from other parts of the same body. It became possible to create artificial implants by evolving material engineering and the development of so-called biomaterials. The use of biomaterials for implant manufacture saw significant growth in the 1960s [1-3]. Several implant classes are based on the medical speciality to which the implants relate, including orthopaedic, cardiac and dental cochlear implants. Some properties are required for all implant classes, such as biocompatibility. As defined in the Williams Dictionary of Biomaterials [4,5], biocompatibility is a material's ability to present an appropriate response in its intended application. In addition to the general characteristics common to all implantable biomaterials, each implant class has specific requirements [6,7].

Any biomaterial in contact with the human body generates a series of responses that should not be harmful to the implanted person's health. These responses include cytotoxicity, of the material, is cytotoxic it causes the death of cells around it; genotoxicity if the material causes chromosomal alteration of the cells around it; and

hemotoxicity if the material causes blood cell death [8,9]. The bio-functionality of a material is its ability to perform its function within a specified period. Orthopaedic implants, due to their primary functional property of long-term mechanical support, need to have excellent mechanical properties of both short and long durations, in addition to the characteristics previously described. Such a need for good mechanical properties initially led to too high an elastic modulus, such as stainless steel, to support the mechanical loads associated with the various types of orthopaedic implants such as hips, knees and spines. The use of materials with a high elastic modulus had harmful consequences, such as the stress-shielding effect [10,11]. The use of highly flexible materials leads to a loss of bone density in the regions around the implant due to Wolf's law, published in the monograph the Law of Bone Transformation [12,13]. Wolf observes that bone density in high mechanical stress regions is elevated more than areas with less mechanical stress. With implants with a high elastic modulus, mechanical loading is transferred from the implant's bone structure.

Several authors report that bone remodelling is highly sensitive to dynamic loads [14,15]. Due to stress-shielding effects, it became necessary to research and develop materials with a lower elastic modulus than metallic materials, combined with high short- and long-term mechanical resistance for orthopaedic implants. Orthopaedic implants are among the most complicated implant classes because they involve almost all parts of the human body [16,17], and nearly all play a role in supporting a mechanical load. The area of spinal implants is one of the most recently developed. It can be divided practically into two sub-classes: spine prostheses, which are implants intended to preserve the functional properties of the original spine structure, that is, to maintain functionality; and implants for spinal arthrodesis, which are used for bone fusion between spine segments to correct instabilities, used if the prosthesis is not feasible [18,19].

The area of spine prostheses is still in an embryonic stage of development, and the volume of use of this type of treatment is minimal. Arthrodesis treatment is the more common approach for spinal instabilities. In these procedures, intervertebral height needs to be maintained. The role of carbon nanotubes and cellular CHAp as scaffold composites in bone tissue production and regeneration is shown in Fig. 1. Height is maintained by implants known as intervertebral cages [20,21]. These devices work as mechanical shims, supporting the intervertebral space and transferring the mechanical load from one vertebra to another. The biomaterial used to produce the vertebral cage must meet a number of functional requirements. Mechanical resistance is the materials ability to undergo mechanical effort, mainly in compression but also bending and shearing. Such loads are exercised cyclically in the walking motion of the human skeleton. Therefore, the mechanical resistance of a material needs to be evaluated in both static and dynamic fatigue, and it must be able to withstand cyclic mechanical effort for at least the period over which the arthrodesis occurs. After this period, the functional properties of the product cease [22,23].

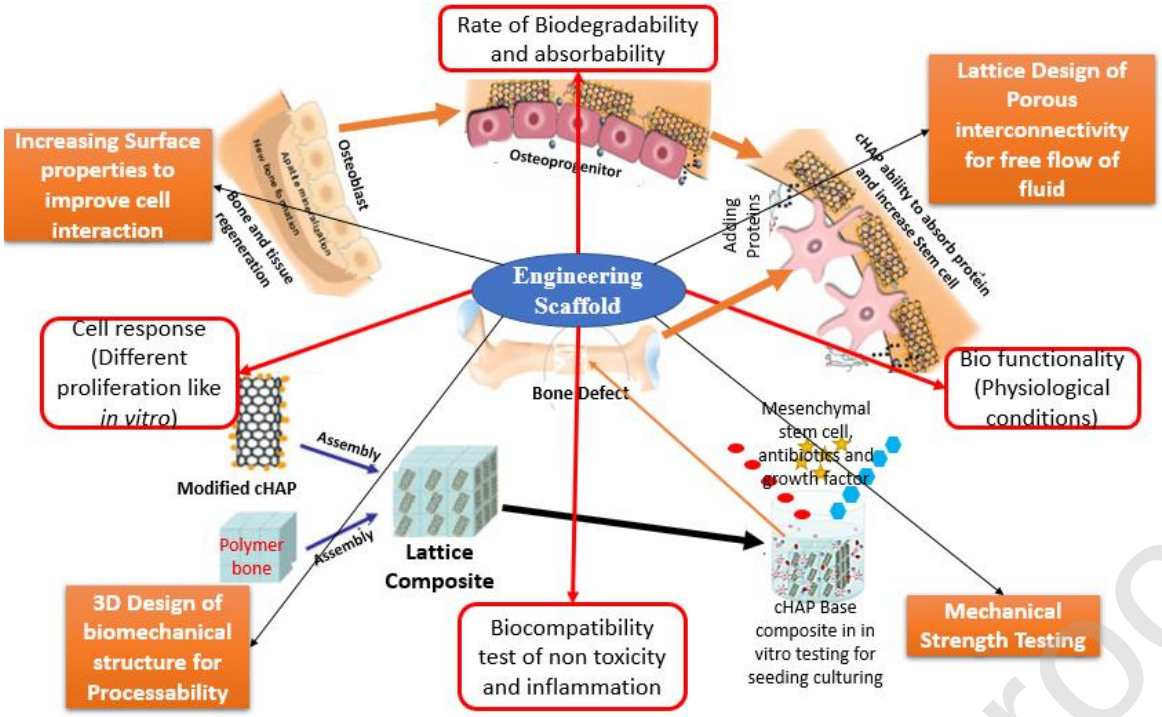

Figure 1. Cell cultures, lattices structure, and seeding for bone tissue engineering and regeneration [20-22]

Osteointegration separates two vertebrae and maintains the intervertebral space until they are joined by bone growth. The biomaterial used must allow for bone growth around it and adapt to its new adjacent structure. Arthrodesis occurs quickly with PEEK as it is a semicrystalline thermoplastic. Therefore it is widely used for mechanical support applications such as spinal, thoracic, lumbar cervical, orthopaedic and trauma implants. It is, therefore, vital to assess the mechanical activity of PEEK in these applications in both the short and long term [24,25]. The mechanical behaviours of semicrystalline thermoplastics are strongly influenced by the degree of polymer crystallinity, the process used, and the final product conditions [26, 27]. This research is standard for the manufacture of technical parts made of semicrystalline thermoplastics used for engineering applications, including surgical implants, to optimise the various transformation processes, such as injection moulding, blow moulding or extrusion. The aim is to increase the degree of crystallinity and minimise internal frozen stresses in the final product for superior performance and mechanical durability. Therefore, this research proposes combining CHAp for bone tissue engineering with state-of-the-art analysis of the 3D printing of PEEK and its composites. The work highlights the optimum 3D printing processes for PEEK and CHAp in various forms, such as powder and filament, the current printing problems and potential applications of 3D printing of PEEK for medical implants.

2. PEEK as a biomaterial

Column implants made of PEEK have relatively recently come into use. The biocompatibility and potential for biomedical applications of PEEK were first reported by Williams, McNamara and Turner [28, 29]. Fig. 2 shows the structure of the PEEK molecule. In the late 1990s, PEEK emerged as a high-performance thermoplastic to replace metal implants and has been commercially supplied for this purpose since April 1998, pioneered by the British manufacturer Invitro [30, 31]. The first application of PEEK as a material for spinal implants was as an

intervertebral cage. The first PEEK intervertebral cage of the type of posterior lumbar interbody fusion (PLIF) was developed in the 1990s by AcroMed. Intervertebral cages made of PEEK overcome two problems caused by conventional metal intervertebral cages stress-shielding caused by the differential elastic modulus between human bone. The implants are radioluminescent, which means they present artefacts under imaging techniques such as X-rays or magnetic resonance, making it impossible to visualise the bone growth in the cages inner region. The invention of intervertebral cells made of PEEK serves as the foundation for its current use in spinal implants [32,33]. Fig. 2 also shows the calcium-based nanomaterials such as CHAp, which are often used to build new bone scaffolds on a PEEK biological macromolecule structure with spinal electrostimulation through a longitudinal axial channel [34, 35].

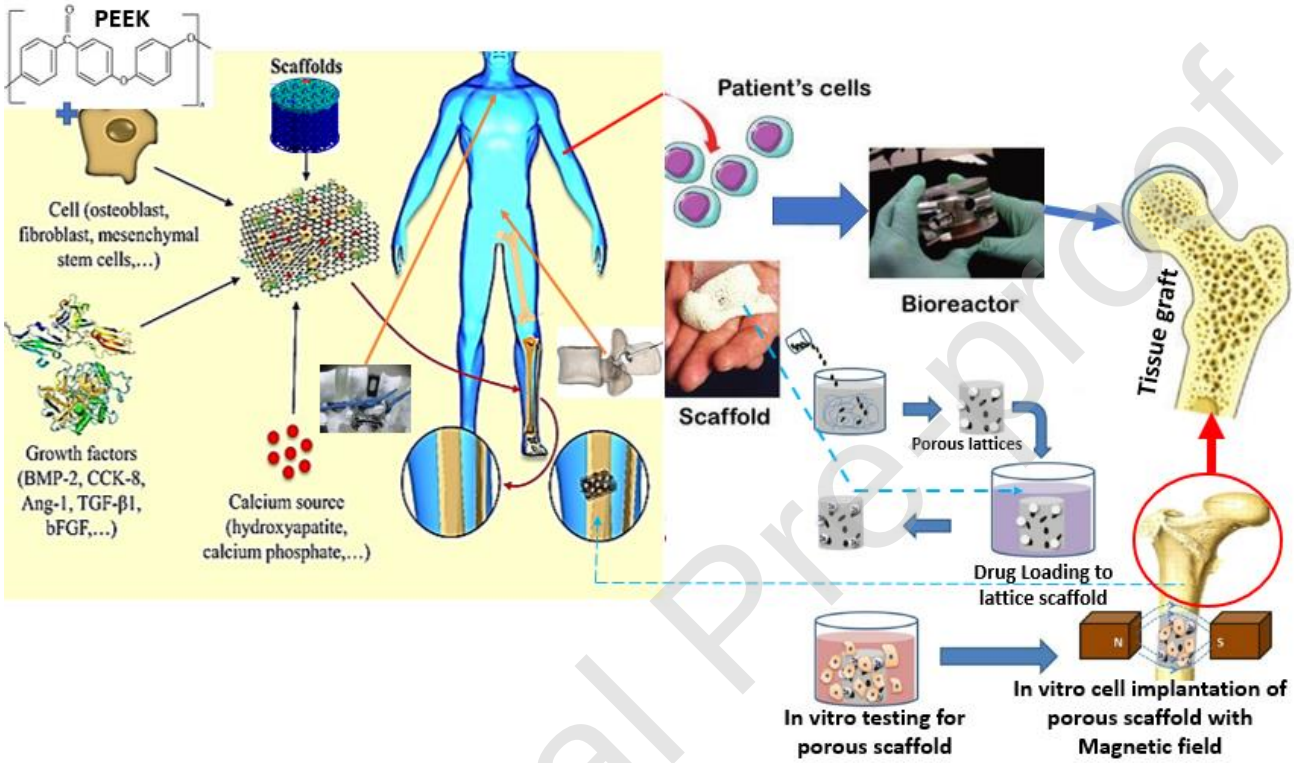

Fig. 2. PEEK biological cellular structure with Brantingan cage, electrostimulation of the spinal with a longitudinal axial channel and lumbar vertebrae[35-37]

The first clinical studies on intervertebral cages of PEEK were carried out on a group of 26 patients who were monitored over two years. Of these, 21 surgeries were successful in terms of the consolidation of arthrodesis, and the five unsuccessful surgeries failed for reasons unrelated to the cages. It was possible to follow up the surgeries using X-ray imaging due to PEEK's radiolucency. This research demonstrates PEEK's biomechanical efficiency as a material suitable for intervertebral cages and post-surgical follow-up ease. The osteointegration capacity of PEEK has been compared to titanium, a metal used in traditional metal cages. Researchers [35-37] have compared PEEK to titanium substrates using various manufacturing processes, such as bar machining and injection moulding. The authors verify, in vitro, that the adhesion of osteoblasts of bone cells is almost the same, with titanium having a slight advantage over PEEK. Injection moulding of PEEK shows results slightly superior to machining [38,39].

2.1. Biological macromolecules of cellular CHAp and its application

Unlike synthetic CHAp, biological cells of CHAp have several impurities. These impurities come about

because the apatite structure allows for replacing a series of ions present in the human body, such as sodium and potassium. A comparative table of the composition of biological macromolecules and synthetic CHAp [40, 41] is presented in Table 1. Several biocompatibility studies have been conducted to show the biocompatibility of synthetic biological macromolecules of CHAp [42- 44]. CHAp powder used in implants is standardised by the International Organization for Standardization (ISO), under ISO 13779-1 of implants for surgery - CHAp - Part 1: Ceramic CHAp. The standard defines the minimum percentage of powder crystallinity, at least 95%, the Ca/P ratio from 1.65 to 1.82 and the maximum trace element percentage, as shown in Table 1 [2-48]. The coating method has special rules for the essential powder properties, such as Ca/P ratio and crystallinity.

2.2. Thermomechanical behaviour of CHAp

Surface engineering modification processes usually involve high temperatures. The plasma deposition process, for example, requires 600ºC in the torch [49-51]. At such temperatures, thermal decomposition can occur, altering the phase balance of the CHAp particles, changing parameters such as the crystalline structure, composition and phase morphology. It is widely accepted [51,52] that heating CHAp has three consequences: water evaporation, dehydroxylation and decomposition. CHAp is highly hygroscopic, so water evaporation occurs when heating the CHAp powder due to the adsorbed water. Dehydroxylation occurs in a part of the apatite structure as CHAp gradually loses the hydroxyl (-OH) group. Decomposition only occurs beyond a certain temperature, as CHAp maintains its crystalline structure during dehydroxylation and rehydrates itself on cooling [53,54]. However, upon reaching a critical temperature, irreversible decomposition occurs, leading to the formation of other calcium phosphates, such as beta-tricalcium phosphate (β-TCP) and calcium tetraphosphate (TTCP), both of which turn into calcium oxide. The reactions are given in Eqs. (1-3) [55, 56]. The temperature effect was presented by [57,58], according to Table 2.

Oxyapatite → Calcium triphosphate + Calcium tetraphosphate: $Ca_{10}(PO_4)_6Ox\ x \rightarrow 2Ca_3(PO_4)_2\ (\beta) + Ca_4(PO_4)_2O$ (1)

Calcium triphosphate → Calcium oxide + Phosphorus pentoxide: $Ca_3(PO_4)_2 \rightarrow 3CaO + P_2O_5$ (2)

Calcium tetraphosphate → Calcium oxide + Phosphorus pentoxide: $Ca_4(PO_4)_2O \rightarrow 4CaO + P_2O_5$ (3)

2.3. Thermal processing of CHAP

Thermal spray processes are processes in which particles are accelerated and deposited in a molten or viscous state on a previously prepared substrate. Several thermal spray techniques are currently available. The process involves a pistol that fires melted particles at high temperatures, up to 600ºC, in a plasma state, at high speed towards the substrate [56-58]. The development of this technique began in the 1960s, with further improvements, such as robotic systems, introduced in the 1980s. The thermal energy of the process is provided by high-energy plasma formed inside a gun which consists of a cathode electrode and an anode nozzle separated by a small void. An electric arc is formed between the anode and the cathode, with argon, helium, hydrogen or nitrogen gas ionised at high energy levels to create a plasma flame through the application of direct current to the cathode. This flame is highly unstable and recombines to form a gas, releasing large amounts of thermal energy [59, 60]. The speeds obtained can reach up to 2300m/s.

During the thermal process, particles are fed into the gun flame by the ionising gas and accelerated towards the substrate. The high temperatures between the gun and the substrate exposed to the particles causes them to fuse. The melting point depends on a series of parameters, such as the flame temperature, the particles' location in the flame, the velocity and the particle size. The impact of CHAp particles on polymeric substrates, such as PEEK, can negatively impact the material's fatigue properties. The state of the particles, fused, semi-fused or solid, can generate micro-cracks on the PEEK surface. This could be critical due to its high sensitivity to stress-concentrating effects. High process temperatures and the particle/substrate impact temperature can also be harmful to the material's resistance to mechanical stress in fatigue. Very little scientific information about this influence on the long-term mechanical properties is available [61-64].

2.4. Other Polymers

Due to their structure, other synthetic polymers can be biodegraded in vivo, and metabolic pathways can reabsorb degradation by-products. This property, together with their processability using various techniques such as additive manufacturing and their relatively good mechanical properties, are the main advantages of synthetic polymers. The main disadvantage is their low cellular affinity, making it challenging to colonise structures, especially in early implantation stages. Polylactic acid (PLA) is a biodegradable synthetic aliphatic polyester obtained by the polymerisation of lactic acid. It has high mechanical resistance, biocompatibility and adequate processability. There are many studies of its potential for structures with bone regeneration applications [60, 61]. A schematic diagram of the cell growth in lattice PEEK and CHAp scaffolds is presented in Fig. 3.

One key restriction of this material is the accumulation of its degradation by-products, which are acidic and can cause inflammation of the surrounding tissue. Polyglycolic acid has worse mechanical properties than the PLA, so its use in bone regeneration is limited. However, its copolymer with polylactic acid (PLGA) is a material with an accelerated degradation rate compared to pure PLA, useful for specific applications such as cranial implants in paediatric cases.

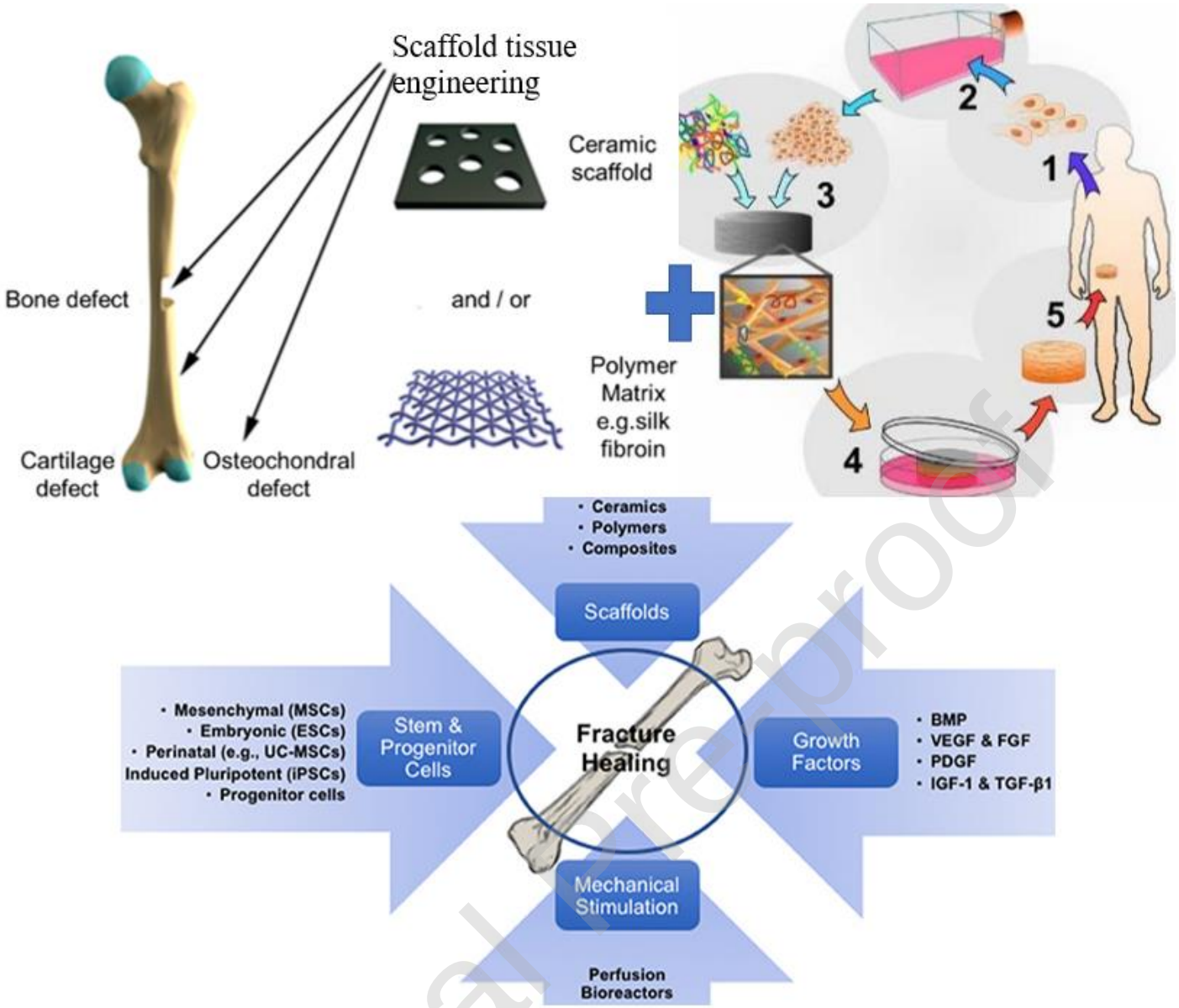

Fig. 3. Schematic of tissue autograft process supported in scaffolds of skeletal tissue regeneration via scaffold-based tissue engineering strategies using a combination of cells, growth factors, and scaffolds. [105-107]

3. PEEK polymer

Despite its macromolecular rigidity, PEEK has considerable flexibility and can withstand high plastic deformation levels in traction and compression. Its stress-strain behaviour exhibits a clear flow transition, as shown in Figs. 4(a) and 4(b), from both tensile and compression tests [65-68]. PEEK exhibits yield stress in compression about 30 to 40% higher than in tension. PEEK is an aromatic thermoplastic that has a high glass transition temperature (Tg) of 143ºC, due to the high rigidity of its macromolecular skeleton. However, its planar zig-zag molecular conformation, despite its high macromolecular rigidity, allows the polymer chains to be arranged in crystalline and amorphous domains. Consequently, PEEK has a crystalline melting point (Tm) of 343ºC. This implies that processing temperatures can vary between 370 and 400ºC, depending on the polymer's molar mass and the type and processing conditions used in manufacturing [69-72]. PEEK's short- and its transition temperature and melting point significantly influence long-term mechanical properties. The properties

of stiffness, strength and toughness of the polymer at in-service temperature have increased the relevance of PEEK in surgical implant applications. Figs. 4(a) and 4(b) show the mechanical behaviour of PEEK under creep in slow deformation as a function of test temperature, in the form of short duration isochronous curves of 100s and curves of creep modulus. The properties of the elastic modulus of short (Fig. 4a) and long (Fig. 4b) duration of PEEK change minimally in the temperature range between 20 and 80ºC [73-75].

As shown in Fig. 4, the use of a higher mould temperature of 200ºC and high injection speed leads to a higher degree of crystallinity of 35% and excellent uniformity throughout the PEEK mould's thickness. These same injection conditions with an increased mould temperature contribute to a higher degree of crystallinity. This gives excellent crystallinity uniformity in various regions in the mould, as shown in Fig. 4. In summary, slower cooling rates, with higher mould temperature of 200ºC, allow PEEK injection moulds to have a higher degree of crystallinity of 30-35%, producing excellent uniformity of crystallinity with less variation of crystallinity in both the thickness and length. PEEK has a crystallisation interval well above room temperature (Tg of 143ºC and Tm of 343ºC), and the higher mould temperature is above the polymer Tg. The longer the polymeric melt resides in this interval, the greater the polymer crystallinity degree [76,79].

As shown in Fig. 4, several authors have investigated the effect of injection speeds between 5.2 and 23.2 cm^2/s on the maximum degree of crystallinity and crystallinity variation across thickness and duration of PEEK. Again, as shown in Fig. 4(a), using the highest mould temperature of 200ºC, the maximum degree of crystallinity can be achieved, and the uniformity across the thickness is practically identical for high and low injection speeds. There is, however, a small advantage to higher injection speeds. Low injection speeds combined with low mould temperatures do not allow the mould cavity to be filled at the highest mould temperature of 200ºC, as shown in Fig. 4 when the degree of variation of crystallinity along the length of the mould is evaluated. Therefore, a combination of a higher mould temperature of 200ºC and a higher injection speed of 23.2 cm^3/s is the moulding condition that allows the maximum degree of crystallinity. This brings excellent uniformity of crystallinity, both through the thickness and length of the PEEK mould.

The same authors evaluate the parts retention time in the mould cavity. They demonstrate that a mould temperature of 150ºC, which is slightly above The PEEK T_g, achieves both full crystallinity and crystallinity uniformity. The thickness and length of the mould tend to increase with the retention time, as shown in Figs. 4(a) and 4(b). Therefore, for a higher mould temperature, above the Tg of semicrystalline thermoplastic, the shorter the time needed to reach a certain degree of crystallinity and uniformity throughout the thickness and length of the moulded PEEK part [86-88].

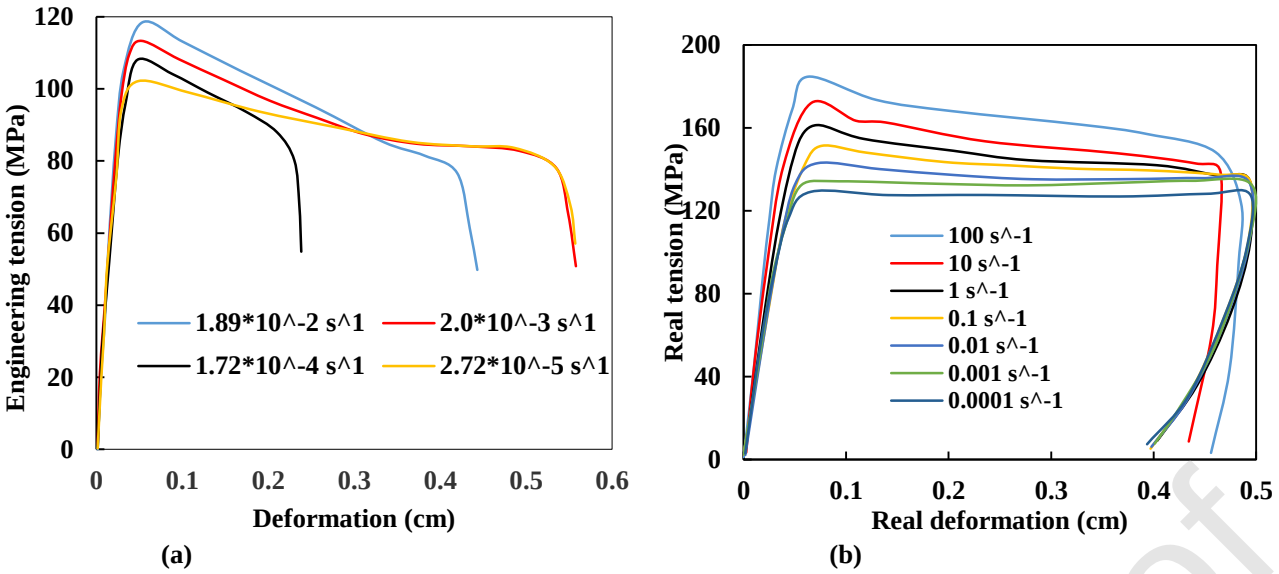

Fig. 4. Stress-strain curve of PEEK in (a) tension and (b) compression for different strain rates

The long-term mechanical stiffness of PEEK is minimally influenced by temperatures that do not exceed 400ºC. The use of PEEK in surgical implants does not exceed this limit since human body temperature is 37ºC, and the long-term mechanical stiffness behaviour of PEEK remains unchanged in these applications in the direction perpendicular to the injection-moulded flow at 90ºC [77-79]. The data in Figs. 4(a) and 4(b) correspond to the creep module property under static mechanical loading. Still, long-term mechanical force of PEEK is influenced by the type of mechanical loading which its products are subject to under specific service conditions. Comparing the two fatigue curves under static and dynamic loads shows that the resistance under dynamic fatigue is always lower than the resistance under static fatigue. The fabrication methods for producing scaffolds using 3D printing and the hierarchical structure of bone indicate that various elements are nanostructured CHAp embedded in collagen fibrils produced from osteoprogenitors and osteoblasts osteoclasts and osteocytes. These are the major cellular constituents of bone in the combination of CHAp and PEEK (fig. 5).

PEEK applications are subject to mechanical loading under a combination of static and cyclic efforts. In surgical implants for the human spine, the dynamic fatigue resistance curve should always establish the structural design calculations stress limits. The endurance limit recorded for a specific type of PEEK is approximately 65MPa, depending on the polymeric material's non-linear viscoelastic nature and its rigidity susceptibility to mechanical hysteresis [81-83]. Other conditions of the fatigue test, such as type and frequency of the request wave, request geometry, test temperature and other relevant parameters, contribute to the expectation that the fatigue strength may change. Considering the failure of plastic materials under mechanical cycling almost always occurs due to crack propagation or fragile failure, it is common to stipulate the design stress value, which incorporates a safety factor above the fatigue resistance limit [84, 85]. As demonstrated in the collected figures and tables, the assessment of PEEK and CHAp's mechanical and thermal-mechanical efficiency is inferred to be closely connected with its crystallinity and uniformity throughout the thickness and length of structural parts.

3.1. PEEK influence and processing conditions

PEEK implants are mainly manufactured in two types of machine-extruded bars or direct injection moulding of implants. Implant manufacturers widely use parts machined from extruded bars, because they use the same machinery to manufacture traditional metal implants, such as machining and turning centres. However, the high cost of implant grade raw materials leads companies to use injection moulding to reduce raw material consumption. The injection moulding process results in greater productivity in the manufacture of complex shaped implants. As explained, the mechanical and other physical properties of PEEK parts are influenced by the level of crystallinity and crystalline morphology.

3.2. PEEK implants compared to others

PEEK has better corrosion resistance than stainless steel, but the mechanical features of PEEK are not optimal for implants' production. Steel is cheaper but less resistant to variations in heat, meaning that during daily use, the fact that the implant efficiently heats and cools negatively affects the patients' life. When the patient is subjected to X-rays, the steel diffuses the radiation, making treatment more complex in terms of doses and targets, such as attacking a cancerous tumour. An implant made of 3D printed PEEK has properties very close to those of human bone in mechanical rigidity and elasticity [87, 88]. PEEK implants synchronise better with the internal movements of bones. Unlike stainless steel, PEEK has insulating properties and therefore undergoes less heat variation. One of the strong points of printed PEEK implants is that they are transparent to X-rays. Table 3 shows methods that can benefit PEEK-based biomedical components and shows some examples of additives referenced in the literature.

According to the injection moulding process thermal cooling cycle, PEEK crystallinity can vary between almost zero and 40%, depending on the moulded part injection mould temperature and thickness. The crystallisation kinetics are slow in crystalline thermoplastic polyethene terephthalate. A crystallisation interval between T_m and T_g, well above room temperature, is associated with its macromolecular skeletons high rigidity. Therefore, in the injection moulding process, regular cooling cycles, the polymer remains for a short time within its crystallisation interval. Table 3 gives the biomedical applications of hydroxyapatite nanocomposites [87-89].

Therefore, with low mould temperatures, a rapid cooling cycle can lead to the manufacture of entirely amorphous and transparent moulded parts of small thicknesses. As the thickness of the cavity increases, pieces are formed with translucent skin and an opaque core of crystalline material under the same rapid cooling conditions. In slow cooling, with increasing mould temperatures, with T_g up to 200ºC, PEEK moulds exhibit good uniformity in the degree of crystallinity throughout the thickness, with minimal variation crystallinity in the skin regions and crumb along the piece length. The thermal process of coating CHAp onto PEEK in biological macromolecular cells is illustrated in Fig. 6 for a 3D printing process of PEEK and CHAP, with a constant melt processing temperatures of 400ºC, a mould temperature ranging between 20 and 200ºC, and injection speeds of 5.2, 13.1 and 23.2 cm^3/s as processing variables [98-100]. Fig. 5 illustrates methods for 3D scaffolding lattices structure.

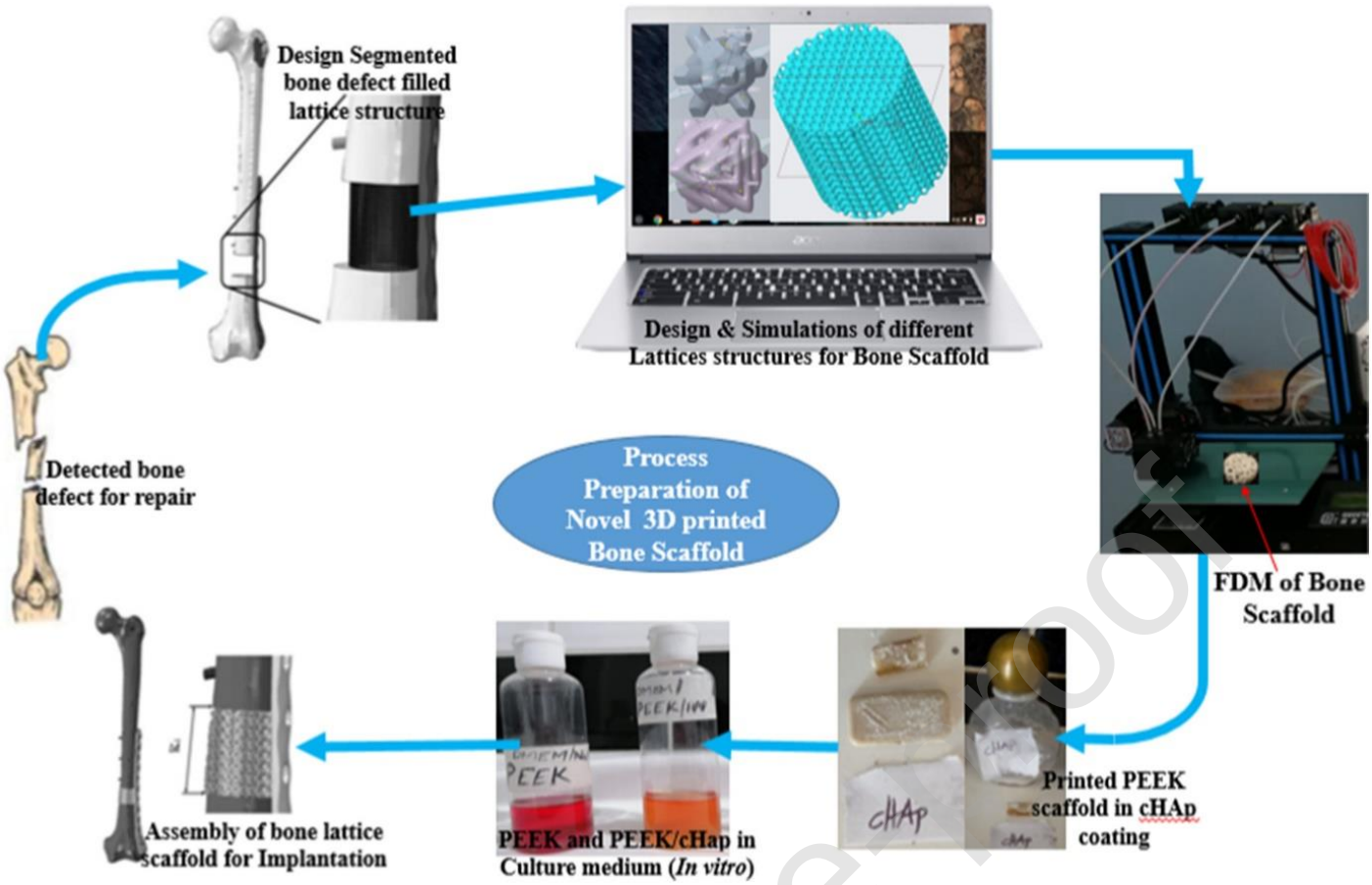

Fig. 5. Strategies for 3D-scaffold architecture of cell growth development of lattice scaffold with cHAP as a composite of PEEK and 3D-printing of scaffolds to create effective bone-implant [2].

4. Concluding remarks

In conclusion, a combination of PEEK and CHAp can be constructed either through composite material coating or extrusion or through multilayer structures. Another alternative to improving the properties of structures used to promote bone regeneration is a surface treatment. The thermal shock impact from the thermal crystallinity process of CHAp on PEEK and the thermomechanical properties are discussed. The manufacturing parameters are compared for injection moulding and coating from the literature. This work reviews the mechanical characteristics of static and dynamic tests and their impacts on PEEK filament mechanical properties after the CHAp coating process. The coating and particle dispersion quality characteristics, morphological analysis of the granulometry, depth of penetration, CHAp layer state after static and dynamic mechanical stresses, and their general applications are discussed. The X-ray diffraction characteristics of CHAp determine whether the thermal process effectively forms a CHAp layer with properties suitable for osteointegration, as revealed by this critical review with parameters preserved in technical and international standards.

In the future, interfacial biological macromolecular cellular studies of CHAp embedded in PEEK and other polymers would benefit biomedical application research, as PEEK and CHAp can be used to repair and replace bone in hard tissues for better support strength. Cellular CHAp with a soft polymer such as PLA fabric maintains skin tissues' functional properties that need flexibility. In tendon repair and cartilage substitution, long-term blood vessels or catheters are required. To meet the current scientific challenges interactions at nano-

biomaterial interfaces must be explored. An accurate understanding of cellular behaviour during exposure to implanted PEEK and CHAp scaffolds is essential to develop safe new techniques for detecting biomolecular interactions. In particular, tissue engineering techniques must consider cell adhesion properties, either for surface enhancement through absorption or the implantation of specific binding factors. The study of biological cellular interfaces of hybrid autonomous cell and bone material has great potential to support biomaterial development.

Ethical statement

The authors declare no ethical issue; the study was conducted in full agreement with ethical standards. Also, the manuscript is neither under review nor published elsewhere.

Declaration of competing interest

We, at this moment, affirm that there is no conflict of interest.

Declaration of interests

The authors declare that they have no known competing for financial interests or personal relationships that could have appeared to influence the work reported in this paper.

References

[1] Rasheva Z, Zhang G, Burkhart TA. Correlation PEEK materials with different fiber orientations. Tribol Int 2010;43:1430–7.

[2] Bankole I. Oladapo, Sikiru O. Ismail, Musa A. Muhammad, Lattice design and 3D-printing of PEEK with Ca10(OH)(PO4)3 and in-vitro bio-composite for bone implant, Inte Jour of Biological Macro Volume 165, Part A, 15 December 2020, Pages 50-62

[3] Bankole I Oladapo, S Abolfazl Zahedi, Sikiru O Ismail, Francis T Omigbodun, Oluwole K Bowoto, Mattew A Olawumi, Musa A Muhammad, 3D printing of PEEK–cHAp scaffold for medical bone implant, Bio-Design and Manufacturing 2021, Pages 44-59

[4] Keul C, Liebermann A. Influence veneering resin composites. J Adhes Dent 2014;16:383-92.

[5] Goyal RK, Tiwari AN, Mulik UP, Negi YS. Dynamic mechanical properties of Al2O3/poly (ether ether ketone) composites. J Appl Polym Sci 2007;104(1):568-75.

[6] M. Tafaoli-Masoule, M Shakeri, SA Zahedi, H Seitz, M Vaezi, 3D printing of PEEK-based medical devices, Transactions on Additive Manufacturing Meets Medicine 2019, 1 (1)

[7] Bankole I Oladapo, S Abolfazl Zahedi, Seng Chong, Francis T Omigbodun, Idowu O Malachi, 3D printing of surface characterisation and finite element analysis improvement of PEEK-HAP-GO in bone implant, The International Journal of Advanced Manufacturing Technology, 2020 Volume 106 (3) Pages 829-841

[8] B. Ashwin, B. Abinaya, T.P. Prasith, S. Viji Chandran, N. Selvamurugan, 3D-poly (lactic acid) scaffolds coated with gelatin and mucic acid for bone tissue engineering, Inter. J. Biol. Macromol., 1621 (2020), pp. 523-532

[9] Oladapo BI, Adeoye AOM, Ismail M. Analytical optimisation of a nanoparticle of microstructural fused deposition of resins for additive manufacturing. Compos Part B Eng 2018;150:248-54.

[10] Lin GM, Xie GY, Sui GX, Yang R. Hybrid effect polymer composites. Compos B Eng. 2012;43(1):44-9.

[11] Wang L, Weng L, Song S, Sun Q. Mechanical properties and microstructure of polyetheretherketone–hydroxyapatite nanocomposite materials. Mater Lett 2010;64(20):2201-4.

[12] Hou X, Shan CX, Choy KL. Microstructures and tribological properties of PEEK-based nanocomposite coatings incorporating inorganic fullerene-like nanoparticles. Surf Coat Technol 2008;202(11):2287-91.

[13] Balla VK, Tadimeti JGD, Kate KH, Satyavolu J. 3D printing of modified soybean hull fiber/polymer composites. Mater Chem Phys 2020;254:123452.

[14] L. Tytgat, L.V. Damme, M.P.O. Arevalo, H. Declercq, S.V. Vlierberghe, Extrusion-based 3D printing of photo-crosslinkable gelatin and κ-carrageenan hydrogel blends for adipose tissue regeneration, Inter. J. Biol. Macromol., 1401 (2019), pp. 929-938

[15] S. Li, SA. Zahedi, V. Silberschmidt, Numerical Simulation of Bone Cutting: Hybrid SPH-FE Approach, Numerical Methods and Advanced Simulation in Biomechanics and Biological Processes, 2017, Pages187-201

[16] Park H-Y, Kim E-H, Cho G-H, Jung Y-G, Jing Zhang J. Process development of fabricating ceramic core using 3D printing technique. Mater Chem Phys 2019;231:382-387.

[17] Adeoye AOM, Kayode JF, Oladapo BI, Afolabi SO. Experimental analysis and optimisation of synthesised magnetic nanoparticles coated with PMAMPC-MNPs for bioengineering application, St. Petersburg Polytech Univ J Phys Math 2017;3:333-8.

[18] Ma, R., Guo, D. Evaluating the bioactivity PEEK biocomposite. J Orthop Surg Res 14, 32 (2019). https://doi.org/10.1186/s13018-019-1069-1

[19] Oliveira TP, Silva SN, Sousa JA. Flexural fatigue behavior of hydroxyapatite-coated polyether-ether-ketone (PEEK) injection moldings derived from dynamic mechanical analysis. Inter J Fatig 2018;108:1-8.

[20] Khurshid Z, Zafar M, Qasim S, Shahab S, Naseem M, AbuReqaiba A. Advances in nanotechnology for restorative dentistry. Materials 2015;8:717-31.

[21] E. Ilhan, S. Cesur, E. Guler, F. Topal, O. Gunduz, Development of Satureja cuneifolia-loaded sodium alginate/polyethylene glycol scaffolds produced by 3D-printing technology as a diabetic wound dressing material, Inter. J. Biol. Macromol., 16115 (2020), pp. 1040-1054

[22] SA Zahedi, C Kodsi, F Berto, Numerical predictions of U-notched sample failure based on a discrete energy argument, Theoretical and Applied Fracture Mechanics, 2019, 100, 298-306

[23] Abdulkareema MH, Abdalsalam AH, Bohan AJ. Influence of chitosan composite coating (PEEK/CHAp) fabricated by electrophoretic deposition. Prog Org Coat 2019;130:251-9.

[24] Kadhim MJ, Abdullatef NE, Abdulkareem MH. Optimisation of nanohydroxyapatite/chitosan electrophoretic deposition on 316L stainless steel using taguchi design of experiments. Al-Nahrain J Eng Sci 2017;20:1215-27.

[25] Najeeb S, Zafar MS,. Applications (PEEK) in oral implantology and prosthodontics. J Prosthod Res 2016;60:12-9.

[26] L. Li, S. Qin, J. Peng, A. Chen, K. Song, Engineering gelatin-based alginate/carbon nanotubes blend

bioink for direct 3D printing of vessel constructs, Inter. J. Biol. Macromol., 14515 (2020), pp. 262-271

[27] SA Zahedi, M Demiral, A Roy, VV Silberschmidt, FE/SPH modelling of orthogonal micro-machining of fcc single crystal, Computational materials science (2013), 78, 104-109

[28] Waser-Althaus J, Salamon A. Differentiation of human PEEK. J Mater Sci Mater Med 2014;25:515-25.

[29] Peng S, Feng P. Graphene oxide PEEK/HAP for tissue engineering scaffolds. Sci Rep 2017;20(7):1-14.

[30] Giannatsis J, Dedoussis V. Additive fabrication health care: A review. Int J Adv Manuf Technol 2009;40(1–2):116-27.

[31] Pakhaliuk V, Poliakov A. Simulation of wear in a spherical joint with a polymeric component of the total hip replacement considering activities of daily living. Facta Univ Ser Mech Eng 2018;16(1):51-63.

[32] Oluwole K Bowoto, Bankole I Oladapo, SA Zahedi, Francis T Omigbodun, Omonigho P Emenuvwe, Analytical modelling of in situ layer-wise defect detection in 3D-printed parts: additive manufacturing, The International Journal of Advanced Manufacturing Technology, 2021, Volume 111 (7) Pages 2311-2321

[33] Y. Liu, R. Wang, S. Chen, Z. Xu, J. Chen, Heparan sulfate loaded polycaprolactone-hydroxyapatite scaffolds with 3D printing for bone defect repair, Inter. J. Biol. Macromol., 1481 (2020), pp. 153-162

[34] Oladapo BI, Zahedi SA, Adeoye AOM. 3D printing of bone scaffolds with hybrid biomaterials Compos Part B Eng 2019;158:428-36.

[35] Wu Z, Liu W, Wu H, Huang R, He R, Jiang Q, Chen Y, Ji X, Tian Z, Wu S. Research into the mechanical properties, sintering mechanism and microstructure evolution of Al2O3-ZrO2 composites fabricated by a stereolithography-based 3D printing method. Mater Chem Phys March 2018;207:1-10.

[36] Oladapo BI, Zahedi SA, Vahidnia F, Ikumapayi OM, Farooq MU. 3D FEA of a porcelain crowned tooth. Beni-Suef Univ J Basic Appl Sci 2019;7:461-4.

[37] Stawarczyk B,. Three-unit reinforced PEEK composite FDPs failure types. Dent .Mater J 2015;34:7-12.

[38] Tytgat L, Damme LV, Arevalo MPO, Declercq H, Vlierberghe SV. Extrusion-based 3D printing of photo-crosslinkable gelatin and κ-carrageenan hydrogel blends for adipose tissue regeneration Inter J Biol Macromol 2019;1401:929-38.

[39] Oladapo BI, Zahedi SA, Chaluvadi SC, Bollapalli SS, Ismail M. Model design of a superconducting quantum interference device of magnetic field sensors for magnetocardiography. Biomed Sig Proc Cont 2019;46:116-20.

[40] Song SY, Park MS, Lee JW, Yun JS. Improvement of agents' coating thickness. Mater Chem Phys 2018;216:446-53.

[41] Oladapo BI, Zahedi SA, Omigbodun FT, Oshin EA, Adebiyi VA, Malachi OB. Microstructural evaluation of aluminium alloy A365 T6 in machining operation. J Mater Res Technol 2019;8:3213-22.

[42] Najeeb S, K. Nano modified peek dental implants: - A review. Int J Dent 2015;2015:1-7.

[43] Godara A, Raabe D, Green S. The Influence of PEEK composites applications. Acta Biomater 2007;3(2):209-20.

[44] Vaezi M, Black C, Gibbs DM, Oreffo RO, Brady M, Moshrefi-Torbati M, Yang S. Characterization of new PEEK/HA composites with 3D HA network fabricated by extrusion freeforming. Molecules 2016;21(6):1-21.

[45] Roskies M, Jordan JO, Fang D, Abdallah MN, Hier MP, Mlynarek A, Tamimi F, Tran SD. Improving

PEEK bioactivity for with mesenchymal stem cells. J Biomater Appl 2016;31(1):132-9.

[46] Zhu Y, Liu X, Yeung KWK, Chu PK, Shuilin W. Biofunctionalization of carbon nanotubes/chitosan hybrids on Ti implants by atom layer deposited ZnO nanostructures. Appl Surf Sci 2017;400:14-23.

[47] Tsai PI, Lam T-N, Wu M-H, Tseng KY, Huang E-W. Multi-scale mapping for collagen-regulated mineralisation in bone remodeling of additive manufacturing porous implants. Mater Chem Phys 2019;230:83-92.

[48] B.C. Maniglia, D.C. Lima, M.D. Matta Junior, P. Le-Bail, P.E.D. Augusto, Hydrogels based on ozonated cassava starch: effect of ozone processing and gelatinisation conditions on enhancing 3D-printing applications, Inter. J. Biol. Macromol., 1381 (2019), pp. 1087-1097

[49] Ranjan N, Singh R, Ahuja IS. Biocompatible thermoplastic composite blended with cHAp and CS for 3D printing. In: Hashmi S, Choudhury LA (Eds.), Ref Mod Mater Sci Mater Eng Encycl Ren Sust Mater 2020;4:379-88.

[50] Hallmann L, Mehl A, Sereno N, Hämmerle CH. The improvement of adhesive properties of PEEK through different pre-treatments. Appl Surf Sci 2012;258(18):7213-8.

[51] Jha S, Bhowmik S, Bhatnagar N, Bhattacharya NK, Deka U, Iqbal HM, Benedictus R. Experimental investigation into the effect of adhesion properties of PEEK modified by atmospheric pressure plasma and low pressure plasma. J Appl Polym Sci 2010;118(1):173-9.

[52] Wakelin EA, Fathi A, Kracica M, Yeo GC, Wise SG, Weiss AS, McCulloch DG, Dehghani F, Mckenzie DR, Bilek MM. Mechanical properties of plasma immersion ion implanted PEEK for bioactivation of medical devices. ACS Appl Mater Interf 2015;7(41):23029-40.

[53] Zafar MS, Ahmed N. Nanoindentation and surface roughness profilometry of poly methyl methacrylate denture base materials. Technol Health Care 2014;22:573-81.

[54] Kong F, Nie Z, Liu Z, Hou S, Ji J. Developments of nano-TiO2 incorporated hydroxyapatite/PEEK composite strut for cervical reconstruction and interbody fusion after corpectomy with anterior plate fixation. J Photochem Photobiol B Biol 2018;187:120-5.

[55] Abdulkareem MH, Abdalsalam AH, Bohan AJ. Influence activity of composite coating (PEEK/CHAp) fabricated by electrophoretic deposition. Prog Org Coat 2019;130:251-9.

[56] Chakravarty J, Rabbi MF, Chalivendra V, Ferreira T, Brigham CJ. Mechanical (PLA)/hydroxyapatite (CHAp) composites cast using ionic liquid solutions. Inter J Biol Macromol 2020;15115:1213-23.

[57] Zalaznik M, Kalin M, Novak S. Influence of the processing temperature on the tribological and mechanical properties of poly-ether-ether-ketone (PEEK) polymer. Tribol Int 2016;94:92-7.

[58] Diez-Pascual AM, Naffakh M, Gómez MA, Marco C, Ellis G, Gonzalez-Dominguez JM, Ansón A, Martinez MT, Martinez-Rubi Y, Simard B, Ashrafi B. The influence of PEEK/carbon nanotube composites. Nanotechnol 2009;20(31):1-13.

[59] Han CM, Lee EJ, Kim HE, Koh YH, Kim KN, Ha Y, Kuh SU. The electron beam deposition of titanium on polyetheretherketone (PEEK) and the resulting enhanced biological properties. Biomater 2010;31(13):3465-70.

[60] Durairaj RB, Borah P, Thuvaragees Y. Characterization of PEEK coated S.S316 l for biomedical application. ARPN J Eng Appl Sci 2015;10:4794-8.

[61] Boonyawan D, Waruriya P, Suttiat K. Characterization of titanium nitride–hydroxyapatite on PEEK for

dental implants by co-axis target magnetron sputtering. Surf Coat Technol 2016;306(Part A):164-70.

[62] Singh S, Prakash C, Ramakrishna S. 3D printing of polyether-ether-ketone for biomedical applications. Europ Polym J 2019;114:234-48.

[63] Prakash J, Prema D, Venkataprasanna KS, Balagangadharan K, Venkatasubbu GD. Nanocomposite chitosan film containing graphene oxide/hydroxyapatite/gold for bone tissue engineering. Inter J Biol Macromol 2020;1541:62-71.

[64] Rong C, Ma G, Zhang S, Song L, Chen Z, Wang G, Ajayan PM. Effect of crystallisation behavior of PEEK. Compos Sci Technol 2010;70(2):380-6.

[65] Petrovic L, Pohle D, Münstedt H, Rechtenwald T, Schlegel KA, Rupprecht S. Effect of βTCP filled polyetheretherketone on osteoblast cell proliferation in vitro. J Biomed Sci 2006;13(1):41-6.

[66] Bijwe J, Sen S, Ghosh A. Influence of PTFE content in PEEK–PTFE blends on mechanical properties and tribo-performance in various wear modes. Wear 2005;258(10):1536-42.

[67] Durham III JW, Montelongo SA, Ong JL, Guda T, Allen MJ, Rabiei A. Hydroxyapatite coating on PEEK implants model. Mater Sci Eng 2016;68:723-31.

[68] Skirbutis G, Dzingutė A, Masiliūnaitė V, Šulcaitė G, Žilinskas J. A review of PEEK polymer's properties and its use in prosthodontics. Stomatologija 2017;19(1):19-23.

[69] Barton AJ, Sagers RD, Pitt WG. Bacterial adhesion to orthopaedic implant polymers. J Biomed Mater Res 1996;30:403-10.

[70] Yu S, Hariram KP, Kumar R, Cheang P, Aik KK. In vitro apatite formation HAP/PEEK biocomposites. Biomater 2005;26:2343-52.

[71] Luo H, Xiong G, Ren K, Raman SR, Wan Y. Air DBD surface coat treatment on three-dimensional braided carbon fiber-reinforced PEEK composites for enhancement of in vitro bioactivity. Surf Coat Technol 2014;242:1-7.

[72] Almasi D, Izman S, Assadian M, Ghanbari M, Abdul Kadir MR. Crystalline ha coating on PEEK via chemical deposition. Appl Surf Sci 2014;314:1034-40.

[73] Omigbodun FT, Oladapo BI, Bowoto OK, Adeyekun FP. Experimental model design and simulation of air conditioning system for energy management. Inter Res J Eng Technol 2019;6:811-6.

[74] Kinbrum A. The PEEK of large joint performance. Orthop Des Technol 2009;3:1-3.

[75] Kurtz SM, Devine JN. PEEK spinal implants. Biomater 2007;28(32):4845-69.

[76] Abu Bakar MS, Cheng MHW, Tang SM, Yu SC, Liao K, Tan CT, Khor KA, Cheang P. Tensile properties, tension-tension fatigue and biological response of polyetheretherketone-hydroxyapatite composites for load-bearing orthopaedic implants. Biomater 2003;24:2245-50.

[77] E.R. Abouzeid, R. Khiari, A. Salama, M. Diab, A. Dufresne, In situ mineralisation of nano-hydroxyapatite on bifunctional cellulose nanofiber/polyvinyl alcohol/sodium alginate hydrogel using 3D printing, Inter. J. Biol. Macromol., 1601 (2020), pp. 538-547

[78] Wong KL, Wong CT, Liu WC, Pan HB, Fong MK, Lam WM, Cheung WL, Tang WM, Chiu KY, Luk KDK, Lu WW. Mechanical strontium-containing HAP/PEEK composites. Biomater 2009;30:3810-7.

[79] Converse GL, Conrad TL, Merrill CH, Roeder RK. Hydroxyapatite whisker reinforced polyetherketoneketone bone ingrowth scaffolds. Acta Biomater 2010;6:856-63.

[80] Chen X, Xu L, Wang Y, Hao Y, Wang L. Image-guided installation of 3D-printed patient-specific

implant and its application in pelvic tumor resection and reconstruction surgery. Comput Meth Prog Biomed 2016;1(125):66-78.

[81] Zhou L, Y Qian Y, Zhu Y, Liu H, Gan K, Guo J. The effect of bond strength of PEEK composite materials. Dent Mater 2014;30:209-15.

[82] Ren Y, Sikder P, Lin B, Bhaduri SB. Microwave assisted coating of bioactive amorphous magnesium phosphate (AMP) on PEEK. Mater Sci Eng C 2018;85:107-13.

[83] Tania Guadalupe Peñaflor Galindo, Yadong Chai, Motohiro Tagaya, "Hydroxyapatite Nanoparticle Coating on Polymer for Constructing Effective Biointeractive Interfaces", Journal of Nanomaterials, vol. 2019, Article ID 6495239, 23 pages, 2019. https://doi.org/10.1155/2019/6495239

[84] Cintia S, Milanie M. Evaluation of the stress distribution in CFR-PEEK dental implants by the three-dimensional finite element method. J Mater Sci Mater Med 2010;21:2079-85.

[85] Briem D, Strametz S, Meenen NM, Lehmann W, Linhart W, Ohl A, Rueger JM. Response of primary (PEEK) surfaces. J Mater Sci Mater Med 2005;6:671-7.

[86] Yu H, Chen Y, Mao M, Liu D, Ai J, Leng W. PEEK-biphasic bioceramic composites promote mandibular defect repair and upregulate BMP-2 expression in rabbits. Mol Med Rep 2018;17:8221-7.

[87] Feng P, Jia J, Peng S, Yang W, Bin S, Shuai C. Graphene oxide-driven interfacial coupling in laser 3D printed PEEK/PVA scaffolds for bone regeneration. Virtual Phys Prototy 2020;15:211-26.

[88] Landy BC, VanGordon SB, McFetridge PS, Sikavitsas VI, Jarman-Smith M. Mechanical and in vitro investigation of a porous PEEK foam for medical device implants. J Appl Biomater Func 2013;11:35-44.

[89] Garcia-Gonzalez D, Rodriguez-Millan M, Rusinek A, Arias A. Low temperature effect on impact energy absorption capability of PEEK composites. Compos Struct 2015;134:440-9.

[90] Durairaj RB, Borah P, Thuvaragees Y. Characterization of PEEK coated S.S316 l for biomedical application. ARPN J Eng Appl Sci 2015;10(11):4794-8.

[91] Almasi D, Izman S, Assadian M, Ghanbari M, Abdul Kadir MR. Crystalline ha coating on PEEK via chemical deposition. Appl Surf Sci 2014;314:1034-40.

[92] Baştan FE, Rehman MAU, Avcu YY, Avcu E, Ustel F, Boccaccini AR. Electrophoretic co-deposition of PEEK-hydroxyapatite composite coatings for biomedical applications. Colloids Surf B Biointerf 2018;169:176-82.

[93] Kurtz SM, Devine JN. PEEK implants. Biomater 2007;28:4845-69.

[94] Williams D. Polyetheretherketone for long-term implantable devices. Med Device Technol 2008;19(1):8-11.

[95] Toth JM, Wang M, Estes BT, Scifert JL, Seim III HB, Turner AS. Polyetheretherketone as a biomaterial for spinal applications. Biomater 2006;27(3):324-34.

[96] Durham III JW, Montelongo SA, Ong JL, Guda T, Allen MJ, Rabiei A. HAP coating on PEEK implants: rabbit model. Mater Sci Eng C 2016;68:723-31.

[97] Zhang C, Zhang G, Vincent JL, Liao H, Costil S, Coddet C. Microstructure and mechanical properties of flame-sprayed PEEK coating remelted by laser process. Prog Org Coat 2009;66:248-53.

[98] Han CM, Lee EJ, Kim HE, Koh YH, Kim KN, Ha Y, Kuh SU. The electron beam deposition of titanium on polyetheretherketone (PEEK) and the resulting enhanced biological properties. Biomater 2010;31:3465-70.

[99] Xing P, Robertson GP, Guiver MD, Mikhailenko SD, Wang K, Kaliaguine S. Synthesis and characterisation of sulfonated PEEK for proton exchange membranes. J Memb Sci 2004;229:95-106.

[100] Sobieraj MC, Kurt SM, Rimnac CM. Notch sensitivity of PEEK in monotonic tension. Biomater 2009;30:6485-94.

Table 1. Constituent chemical elements between biological macromolecules and synthetic, and limited heavy metals [42, 48].

Constituents (fraction by weight) %	**Biological CHAp**	**Synthetic CHAp**	**Element**	**Maximum limit (mg/kg)**
Ca	24.50	39.6	Arsenic	3
P	11.50	18.5	Cadmium	5
Na	0.70	Trace	Mercury	5
K	0.03	Trace	Lead	30
Mg	0.55	Trace		
CO_3^2	5.80	-		

+

Table 2. Thermal effects of CHAp plasma [57,58].

Effect	**Temperature (ºC)**
Evaporation of absorbed water	25 - 600
Decarbonisation	600 - 800
cHAp dehydroxylation, forming	800 - 900
Partially dehydroxylated or completely dehydroxylated	1050 – 1400
AH decomposition, forming β-TCP	< 1120
TTCP	1120 – 1470
β-TCP is stable	1550
β-TCP is converted to α-TCP	1630
CHAp fusion temperature	1730

Table 3 Comparison of high-performance PEEK composite-based biomedical devices and . Methods of improving PEEK's quality characteristics

PEEK composite	Processing method	Mechanical Properties	Application	Description and Results
Nano-TiO2/PEEK [78-80]	Mixing of powder and compression at 400°C	3.8 GPa bending module and 93 MPa bending power	Bone substitution	The bioactivity of the end product with a nano-TiO2 filling improved significantly.
Nano-HAp/PEEK [80-82]	380°C compression and powder mixing	4.6 MPa elastic module and 160 MPa compression power	Orthopaedic implants	The composites nano-HAp/PEEK have been discovered to facilitate cell attachment, propagation, proliferation and osteogenic.
BioHPP [82-84]	Wax moulding at 400°C	–	Dental prosthesis	The replacement for traditional metallic materials should not be considered BioHPP
HAP embedded PEEK [84-86]	Moulding and chemical liquidation of compression	–	Interbody spinal fusion	For the backbone applications, the resulting material is promising
PEEK blanks [86-88]	Acid etching and silica coating are the techniques used for milling.	14.5 ± 2.6 MPa	Dental prosthesis	Silica PEEK coated has enhanced mechanical properties
PEEK [83-85]	Mould and soak with 400°C phosphates buffered saline	The average maximum load is 1790 N	Orthopaedic	Soak does not affect PEEK
Knitted carbon/PEEK [86-88]	Micro-braiding yarn and hot moulding at 380°C	–	Fixations Orthopedic	There was more excellent deformability in knitted composition bone plates.
Chitosan/PEEK [87-89]	Air plasma modification	–	Regenerative medicine	The antibacterial properties of Chitosan led to polymer
PEEK PSIs [90-92]	–	–	Facial Maxillo-Operation	There were no risks to the materials.
PEEK films [93-95]	Moulding compression and treatment of NAOH at 180°C	–	Ophthalmology	The creation of the PEEK apatite layer has been extended
PEEK [95-97]	CNC machine	–	Treatment of Skull Bone	The findings supported the use of PEEK
PEEK/Alumina [20-22]	Composite fabrication	Mechanical		PEEK/Alumina improved the dynamic strength by 78%.
PEEK/Hap [22-24]		Mechanical	Bone implant and Dental prosthesis	Due to good interactivity between HAp and PEEK, the tensile strength of the composite was increased.
PEEK/Carbon nano-tubes [24-27]		Mechanical and crystalline	Tissue engineering	The reinforcement improved the mechanical characteristics and decreased PEEK crystallisation rate.
PEEK/β-TCP[27-30]		Biological cell	Tissue engineering	The growth rates in β-TCP/PEEK osteoblast cells were below PEEK.
Titanium [30-32]	Electron beam deposition	Biological	Tissue engineering and Bone implant	In-vivo studies have shown the enhanced contact ratio between bones and PEEK implants due to titanium coating.
PEEK/ Polytetrafluoroethylene [32-38]	Blending	Tribological	Automobile	The friction coefficient was reduced with the use of polytetrafluoroethylene in PEEK
	Plasma Immersion ion deposition	Biological	Interbody spinal fusion	The tested technique helps improvment of orthopaedic implants in the next decade
PEEK, PEKK [39-42]	Plasma treatment	Chemical	Tissue engineering	The PEEK atmospheric pressure plasma treatment performed remarkably towards improving the stickiness of the polymer